



Original article

Design and synthesis of antifungal benzoheterocyclic derivatives by scaffold hopping

Chunquan Sheng¹, Xiaoying Che¹, Wenya Wang, Shengzheng Wang, Yongbing Cao, Jianzhong Yao, Zhenyuan Miao^{**}, Wannian Zhang^{*}

School of Pharmacy, Second Military Medical University, 325 Guohe Road, Shanghai 200433, People's Republic of China

ARTICLE INFO

Article history:

Received 31 October 2010

Received in revised form

13 January 2011

Accepted 17 January 2011

Available online 22 February 2011

Keywords:

Non-azole lead

CYP51

Scaffold hopping

Benzoheterocyclic derivatives antifungal activity

Molecular docking

ABSTRACT

The incidence of invasive fungal infections and associated mortality is increasing dramatically. Although azoles are first-line antifungal agents, cross-resistance and hepatic toxicity are their two major limitations. The discovery of novel non-azole lead compounds will be helpful to overcome these problems. On the basis of our previously reported benzopyran non-azole CYP51 inhibitor, scaffold hopping was used to design structurally diverse new compounds and expand the structure–activity relationships of the lead structure. Five kinds of scaffolds, namely benzimidazole, benzoxazole, benzothiazole, quinoxalin-4-one and carboline, were chosen for synthesis. In vitro antifungal activity data and results from molecular docking revealed that the scaffold was important for the antifungal activity. Several compounds showed potent activity against both standard and clinically resistant fungal pathogens, suggesting that they can serve as a good starting point for the discovery of novel antifungal agents.

© 2011 Elsevier Masson SAS. All rights reserved.

1. Introduction

Systemic and invasive fungal infections are often life-threatening and have become increasingly common in the immunocompromised hosts, such as patients undergoing anticancer chemotherapy or organ transplants and patients with AIDS [1,2]. Azole antifungal agents were broadly used as the first-line drugs in clinic because of their high therapeutic index. They act by competitive inhibition of the lanosterol 14 α -demethylase (CYP51), a key enzyme in ergosterol biosynthesis pathway of fungal cell membrane [3]. Azole antifungal agents inhibit CYP51 through the formation of a coordination bond between the heterocyclic nitrogen atom (N-3 of imidazole and N-4 of triazole) and the heme iron atom in the active site of the enzyme [4]. However, the azole pharmacophore is also responsible for the hepatotoxicity of azole antifungal agents, because of the coordination binding of its nitrogen atom to the heme of a lot of host cytochrome P450 enzymes (particularly mammalian CYP3A4) [5]. Moreover, the

extensive use of azole antifungal agents has led to severe resistance, which significantly limited the efficacy of them [6]. This situation prompted us to search novel non-azole lead compounds with more structural specificity for the fungal CYP51 enzymes and separate their activity from toxicity.

In our previous studies, three-dimensional (3D) models of CYP51 was constructed using homology modeling [7–10]. Furthermore, we reported the first example of structure-based *de novo* design of novel non-azole CYP51 inhibitors [11]. The benzopyran inhibitors (Fig. 1) were bound to CYP51 mainly through non-bond interactions without coordinating with the heme [11], which representing a promising class of lead structures for the development of selective antifungal agents without cross inhibiting other cytochrome P450 proteins. Therefore, the extension of structure–activity relationships (SARs) of these CYP51 inhibitors is of great importance. Herein, a series of benzoheterocyclic derivatives were designed and synthesized by scaffold hopping. In vitro antifungal activity assay indicated that several compounds showed improved antifungal activity.

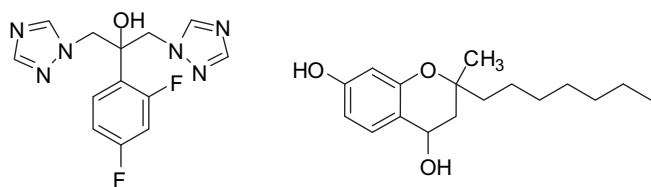
2. Chemistry

The synthetic route of target compounds was outlined in Scheme 1 and Scheme 2. In general, the target compounds were

* Corresponding author. Tel./fax: +86 21 81870243.

** Corresponding author. Tel./fax: +86 21 81871233.

E-mail addresses: miaozhenyuan@hotmail.com (Z. Miao), zhangwnk@hotmail.com (W. Zhang).¹ These two authors contributed equally to this work.



Fluconazole

Non-azole CYP51 Inhibitor

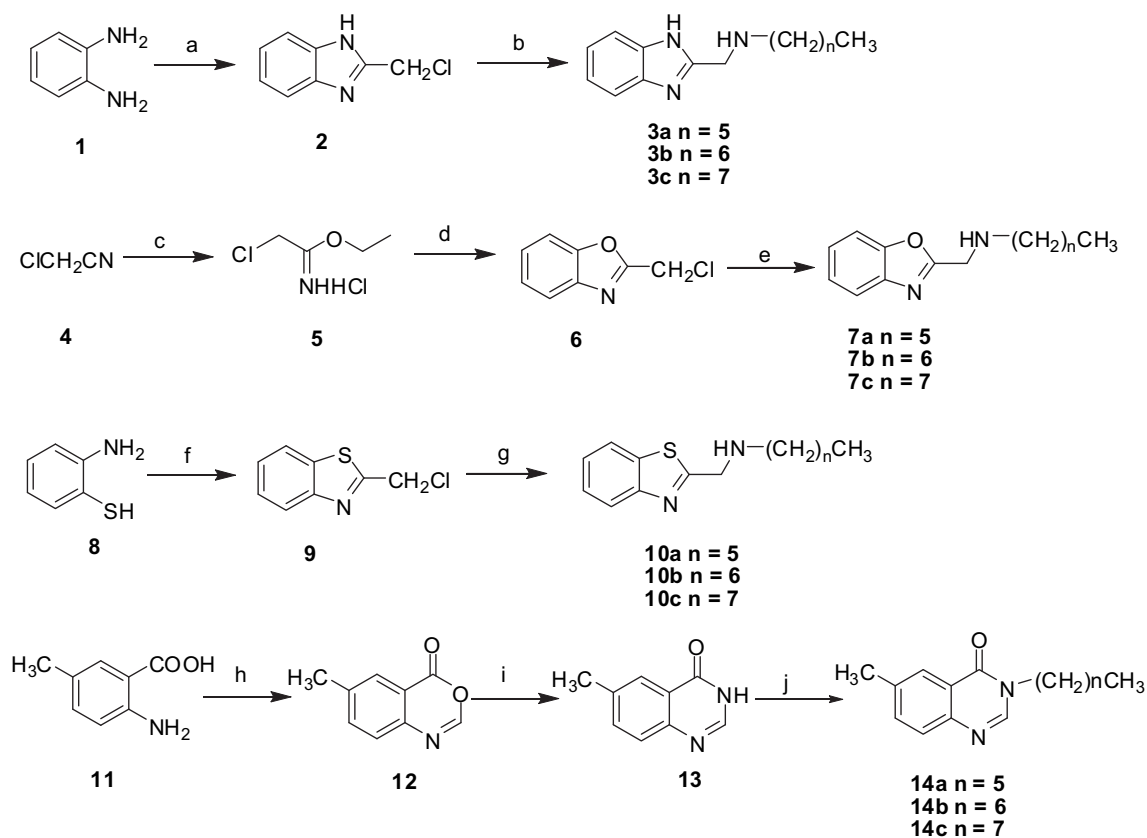
Fig. 1. Chemical structures of representative CYP51 inhibitors.

obtained via a two-step strategy. First, the benzoheterocyclic scaffold was constructed by various ring closure reactions. Then, the alkyl side chains were substituted on the scaffold to afford the target compounds. Benzene-1,2-diamine and ethyl chloroacetate were condensed in dilute HCl solution to afford 2-(chloromethyl)-1H-benzimidazole (**2**). In the presence of K_2CO_3 , scaffold **2** was substituted by various 1-bromide alkylamines in MeOH at room temperature to give compounds **3a–c**. 2-Chloroacetonitrile (**4**) was transformed to ethyl 2-chloroacetimidate (**5**) by reacting with diethyl ether in absolute EtOH at 0 °C. Compound **5** was condensed with 2-aminophenol and 2-aminobenzenethiol in CH_2Cl_2 to afford 2-(chloromethyl)benzoxazole (**6**) and 2-(chloromethyl)benzothiazole (**9**), respectively. Target compounds **7a–c** and **10a–c** were obtained by a similar procedure with **3a–c**. 2-amino-5-methylbenzoic acid (**11**) was treated with formic anhydride to afford benzoxazin-4-one **12**, which was subsequently reacted with formamide at 150 °C to give quinazolin-4-one **13**. Compounds

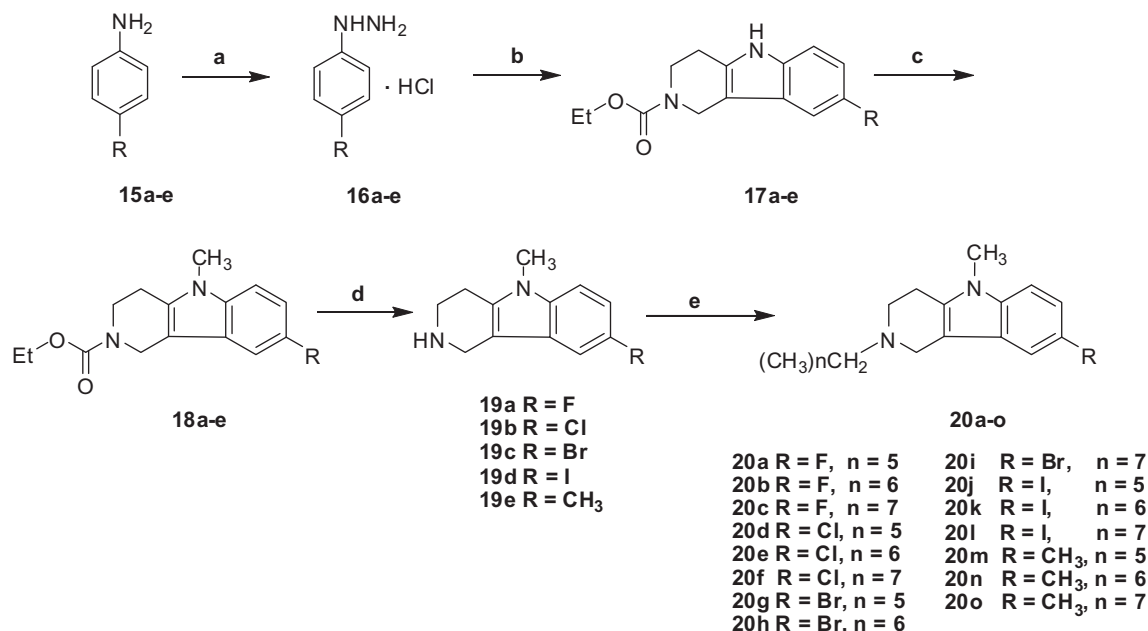
14a–c were obtained by reacting **13** with various 1-bromoalkanes in the presence of NaH and DMF at 80 °C. γ -Carboline derivatives **17a–e** were prepared following the standard Fischer synthesis from substituted phenylhydrazines **16a–e** and *N*-carboxy-4-piperidinone [12,13]. Free NH of **16a–e** was treated with excess iodomethane in the presence of KOH and DMF to give **18a–e**. Then, the *N*-carboxy group of **18a–e** was removed by hydrolysis reaction using KOH/EtOH condition. Finally, carbolines **19a–e** were substituted with various 1-bromoalkanes in the presence of K_2CO_3 and EtOH at 80 °C to afford the title compounds **20a–o**.

3. Pharmacology

In vitro antifungal activity was measured according to the National Committee for Clinical Laboratory Standards (NCCLS) recommendations. The antifungal activity of the target compounds was expressed as the minimal inhibitory concentration (MIC) that achieved 80% inhibition of the tested fungi using fluconazole as a reference drug. The MIC determination was performed by means of the serial dilution method in 96-well microtest plates with RPMI 1640 (Sigma) buffered with 0.165 M MOPS (Sigma) as the test medium. Fluconazole was used as the reference drug. Tested fungal strains were obtained from the ATCC or were clinical isolates. The MIC value was defined as the lowest concentration of test compounds that resulted in a culture with turbidity less than or equal to 80% inhibition when compared to the growth of the control. Test compounds were dissolved in DMSO serially diluted in growth medium. The yeasts were incubated at 35 °C, and the



Scheme 1. Reagents and conditions: a. ethyl chloroacetate, dilute HCl solution, rt~110 °C, 8h, 79.16%; b. 1-bromide alkylamine, K_2CO_3 , MeOH, rt, 10–30min, 10–20%; c. absolute EtOH, HCl (g), diethyl ether, 0 °C, 5.5h, 81.47%; d. 2-aminophenol, CH_2Cl_2 , 0 °C~rt, 99.5%; e. 1-bromide alkylamine, K_2CO_3 , MeOH, rt, 10–30min 10–25%; f. 2-aminobenzenethiol, CH_2Cl_2 , 0 °C~rt, 67.8%; g. 1-bromide alkylamine, K_2CO_3 , MeOH, rt, 10–30min, 15–20%; h. formic anhydride, reflux, 5h, 68.2%; i. formamide, 150 °C, 7h, 75.5%; j. 1-bromoalkane, NaH, DMF, 80 °C, 8h, 85%.



Scheme 2. Reagents and conditions: **a.** sodium nitrite, hydrochloric acid, water, $\text{SnCl}_2 \cdot 2\text{H}_2\text{O}$, -5 – -20 °C, 45 min, 50.5%–75.2%; **b.** ethyl 4-oxopiperidine-1-carboxylate, alcohol, 80 °C, 4h, 45%–50%; **c.** CH_3I , KOH, DMF, 30 °C, 10h, 13.3%–62.6%; **d.** KOH, alcohol, water, 80 °C, 10h, 49.4–81.8%; **e.** 1-bromoalkane, K_2CO_3 , alcohol, 80 °C, 14.2%–25%.

growth MIC was determined at 24 h for *Candida* species, at 72 h for *C. neoformans*, and at 7 days for filamentous fungi.

4. Results and discussion

4.1. Design rationale

Previous modeling studies revealed that the active site of CACYP51 could be divided into four pockets (S1–S4) [11]. S1 subsite is a hydrophilic hydrogen bond binding pocket, while S2 subsite is above the heme ring representing the core hydrophobic area. S3 and S4 subsite represent a narrow and hydrophobic cleft (facing BC loop) and a hydrophobic hydrogen bond binding site (facing FG loop), respectively. The binding mode of the benzopyran lead compound indicated that the core scaffold was located in S2 subsite with its long alkyl side chain oriented into the hydrophobic S3 subsite. The SARs of the substitutions on the benzopyran ring and the length of alkyl side chain have been investigated [11]. Interestingly, the replacement of the benzopyran scaffold by the tetrahydroquinoline ring led to the increase of the antifungal activity [14], which encouraged us to expand the SARs of the scaffold. Scaffold hopping is a useful method to discover structurally novel compounds by modifying the central core structure of the known active compounds [15]. In consideration of synthetic accessibility, we designed five kinds of scaffolds (*i.e.* benzimidazole, benzoxazole, benzothiazole, quinazolin-4-one and carboline) for synthesis (Fig. 2). Based on our previous SAR results, the length of side chains was set to 6 to 8 carbon atoms. As a result, a series of benzoheterocyclic derivatives with long alkyl side chains were synthesized.

4.2. In vitro antifungal activities and SARs

The antifungal activity of the target compounds was shown in Table 1 and Table 2. Benzimidazole derivative **3a** showed potent activity against *C. albicans* ($\text{MIC}_{80} = 1$ $\mu\text{g/mL}$), which was comparable to fluconazole. However, its antifungal spectrum was narrow because it was inactive against other tested pathogenic fungi.

Compounds **3b** and **3c** have longer alkyl side chain and their activity against *C. albicans* was lower than that of **3a**. Interestingly, they showed improved activity against a fluconazole-resistant strain with their MIC_{80} values of 32 $\mu\text{g/mL}$ and 16 $\mu\text{g/mL}$, respectively. Moreover, compound **3c** showed broad antifungal spectrum. Its MIC_{80} value against *C. neoformans*, *C. tropicalis*, *T. rubrum*, *M. gypseum* and *A. fumigatus* was 16 $\mu\text{g/mL}$. Especially, compound **3c** showed moderate activity against *A. fumigatus* ($\text{MIC}_{80} = 32$ $\mu\text{g/mL}$), while fluconazole was inactive. Benzoxazole derivatives **7a–c** revealed moderate to good activities against most of the tested fungi with their MIC_{80} values in the range of 1 $\mu\text{g/mL}$ to 64 $\mu\text{g/mL}$. The activity of compound **7c** against *C. neoformans* ($\text{MIC}_{80} = 1$ $\mu\text{g/mL}$) and *T. rubrum* ($\text{MIC}_{80} = 4$ $\mu\text{g/mL}$) was comparable to that of fluconazole. Moreover, it showed higher activity against *M. gypseum* ($\text{MIC}_{80} = 8$ $\mu\text{g/mL}$) than fluconazole. When the benzoxazole scaffold of **7a–c** was replaced by benzothiazole, the antifungal activity was slightly decreased. The MIC_{80} range of compounds **10a–c** is 16 $\mu\text{g/mL}$ to 32 $\mu\text{g/mL}$. The loss of antifungal activity was observed for quinazolinone derivatives **14a–c**. Only compound **14b** showed moderate activity against *A. fumigatus* ($\text{MIC}_{80} = 64$ $\mu\text{g/mL}$). For carboline derivatives **20a–o**, 8-F (**20a–c**), 8-Cl (**20d–f**), 8-Br (**20g–i**) and 8-I (**20j–l**) analogs only showed marginal antifungal activities. On the other hand, the antifungal activity of 8-methyl derivatives **20m–o** was improved. They showed broad spectrum with MIC_{80} values in the range of 16 $\mu\text{g/mL}$ to 64 $\mu\text{g/mL}$. Especially, compounds **8n** and **8o** revealed the highest activity against *A. fumigatus* ($\text{MIC}_{80} = 16$ $\mu\text{g/mL}$).

From the antifungal activity data, preliminary SARs of the synthesized compounds are obtained as follows. In general, the chemical scaffold of the designed compounds is important for their antifungal activity. Benzimidazole and benzoxazole are found to be favorable for the antifungal activity. Benzimidazole derivative **3a** showed the highest activity against *C. albicans*. On the *C. neoformans* strain, benzoxazole derivative **7c** is the most active. The effect of the length of alkyl side chain on the antifungal activity is not obvious. The introduction of quinazolinone scaffold leads to the loss of antifungal activity. For the carboline derivatives, the substitutions on the C-8 position phenyl ring play an important role for their antifungal

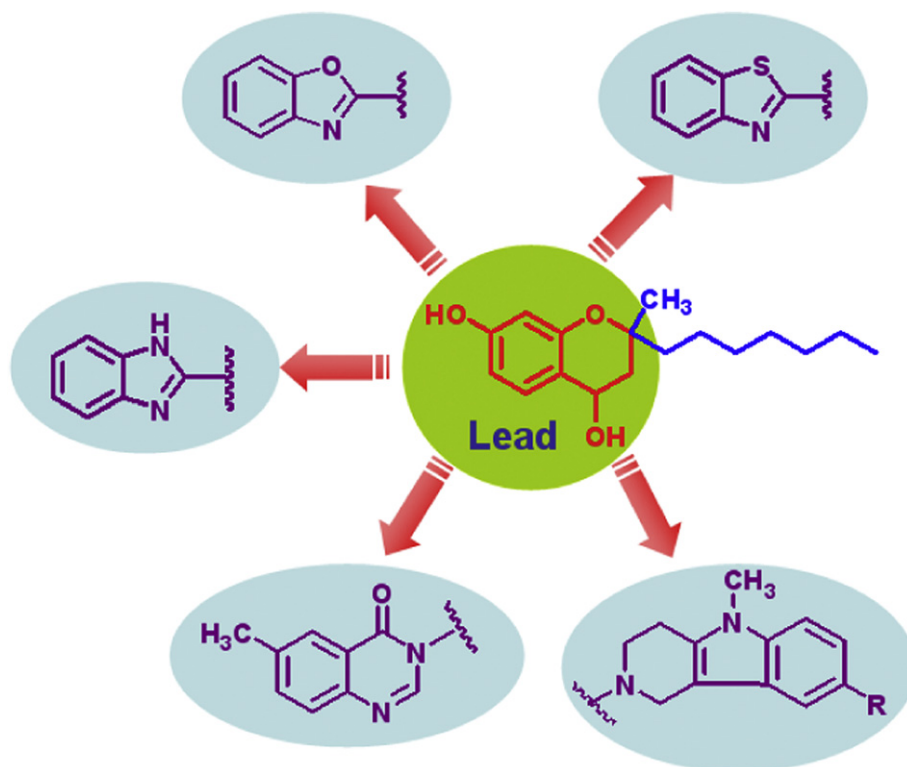


Fig. 2. Scaffold hopping of benzopyran non-azole CYP51 inhibitors.

activity. Most of the halogen substituted compounds are found to be inactive. Among them, only iodine derivative **20i** showed marginal activity. The methyl group seems to be the most favorable. Compounds **20m–o** show improved antifungal activity and spectrum.

4.3. Binding mode of the compounds

In an attempt to understand the binding mode of the designed compounds, representative active derivative **3a** was docked into the active site of CACYP51 using the Affinity module within InsightII 2000 software package [16]. As shown in Fig. 3, the benzimidazole core of compound **3a** was located above the heme ring and formed hydrophobic interactions with the surrounding residues lined with Phe145, Leu139, Ile304 and Phe145. The imidazole NH formed a hydrogen bond with backbone carbonyl oxygen atom of Met306. The long alkyl side chain formed hydrophobic and *van der Waals*

interactions with Phe228, Met306, Leu376 and Val509. Among the designed scaffolds, only benzimidazole has a free NH group to form hydrogen-bonding interaction with Met306. The replacement of benzimidazole by other benzoheterocyclic led to the decreased activity against *C. albicans*. Therefore, the hydrogen bonding interaction with CACYP51 might important for the antifungal activity. On the other hand, the scaffold of the designed compounds was located in a hydrophobic environment. Hydrophobic substitutions on the scaffold could improve the binding affinity with CACYP51. The hypothesis was supported by the SAR of the carboline

Table 1
In vitro antifungal activities of the compounds (MIC_{80} , $\mu\text{g}\cdot\text{mL}^{-1}$).^a

Compd.	<i>C. alb</i>	<i>C. neo</i>	<i>C. tro</i>	<i>T. rub</i>	<i>A. fum</i>	<i>M. gyp</i>	<i>C. alb</i> ^b
3a	1	>64	>64	64	>64	>64	>64
3b	>64	64	>64	64	>64	>64	32
3c	>64	16	16	16	32	16	16
7a	64	64	64	16	>64	16	>64
7b	64	16	64	16	64	16	64
7c	64	1	16	4	32	8	64
10a	64	64	64	64	>64	64	64
10b	64	64	64	16	>64	16	32
10c	64	16	64	16	>64	64	>64
FLZ	1	1	1	4	>64	16	–

^a Abbreviations: *C. alb.* *Candida albicans*; *C. neo.* *Cryptococcus neoformans*; *C. tro.* *Candida tropicalis*; *T. rub.* *Trichophyton rubrum*; *A. fum.* *Aspergillus fumigatus*; *M. gyp.* *Microsporium gypseum*; FLZ: Fluconazole.

^b Clinical isolate resistant to FLZ.

Table 2
In vitro antifungal activities of the compounds (MIC_{80} , $\mu\text{g}\cdot\text{mL}^{-1}$).^a

Compd.	<i>C. alb</i>	<i>C. par</i>	<i>C. kru</i>	<i>C. tro</i>	<i>C. neo</i>	<i>A. fum</i>
14a	>64	>64	>64	>64	>64	>64
14b	>64	>64	>64	>64	>64	64
14c	>64	>64	>64	>64	>64	>64
20a	>64	>64	>64	>64	>64	>64
20b	64	64	>64	>64	>64	64
20c	64	64	>64	>64	>64	>64
20d	>64	>64	64	>64	>64	64
20e	>64	>64	>64	>64	>64	>64
20f	>64	64	64	>64	>64	>64
20g	>64	>64	>64	>64	>64	64
20h	>64	64	>64	>64	64	>64
20i	64	16	>64	>64	64	>64
20j	>64	64	>64	>64	>64	>64
20k	>64	64	>64	>64	>64	>64
20l	64	16	64	>64	>64	>64
20m	64	64	16	64	64	64
20n	16	16	64	64	>64	16
20o	16	16	64	64	>64	16
FLZ	1	1	0.5	1	1	>64

^a Abbreviations: *C. alb.* *Candida albicans*; *C. neo.* *Cryptococcus neoformans*; *C. tro.* *Candida tropicalis*; *T. rub.* *Trichophyton rubrum*; *A. fum.* *Aspergillus fumigatus*; *M. gyp.* *Microsporium gypseum*; FLZ: Fluconazole.

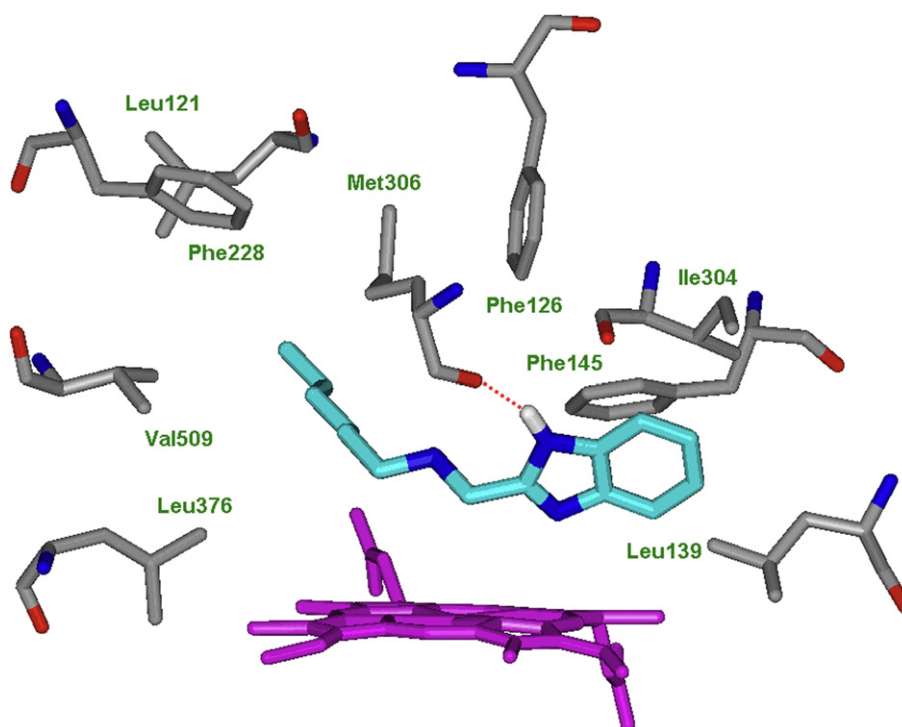


Fig. 3. The binding mode of compound **3a** with the active site of CYP51. Important residues involved in inhibitor binding are shown in stick mode and the hydrogen bond was depicted as red dotted line. The heme atoms are colored purple, the nitrogen atoms are colored blue, the oxygen atoms are colored red, and the carbon atoms are colored gray (CYP51) and cyan (inhibitor). (For interpretation of the references to colour in this figure legend, the reader is referred to the web version of this article.)

compounds **20a–o**. The methyl substituted derivatives showed better activity against *C. albicans* than the corresponding halogen substituted compounds.

5. Conclusion

Cross-resistance and hepatic toxicity are two major limitations for azole antifungal agents. The discovery of novel non-azole CYP51 inhibitors is great significance to overcome these problems. Starting from our previously designed non-azole lead structure, scaffold hopping was used to design structurally diverse antifungal benzo-heterocyclic derivatives. SAR of the lead structure was further extended. Moreover, the synthesized non-azole antifungal compounds have several advantages. (1) They bound with CYP51 through non-bond interactions without coordination to the iron atom, which is helpful to reduce the toxicity of azoles due to cross inhibition of other cytochrome P450 proteins. (2) As compared with the lead structure, several compounds (e.g. **3a** and **7c**) showed improved antifungal activity, which can serve as a good starting point for further optimization. (3) Several compounds were active against fluconazole-resistant clinical isolates, which affords an opportunity to overcome the emerging severe resistance of azoles. Further structural optimization studies are in progress.

6. Experimental protocols

6.1. General procedure for the synthesis of compounds

Nuclear magnetic resonance (NMR) spectra were recorded on a Bruker 500 spectrometer with TMS as an internal standard and CDCl_3 as solvent. Chemical shifts (δ values) and coupling constants (J values) are given in ppm and Hz, respectively. ESI mass spectra were performed on an API-3000 LC–MS spectrometer. High-resolution mass spectrometry measurements were performed on

a Kratos-concept mass spectrometer under electron impact ionization (EI) conditions. TLC analysis was carried out on silica gel plates GF254 (Qindao Haiyang Chemical, China). Silica gel column chromatography was performed with Silica gel 60 G (Qindao Haiyang Chemical, China). Commercial solvents were used without any pretreatment.

6.1.1. Chemical synthesis of 2-(chloromethyl)-1H-benzimidazole (**2**)

A solution of benzene-1,2-diamine (10.8 g, 0.10 mol) and ethyl chloroacetate (15.9 g, 0.13 mol) in dilute HCl solution (4 M, 90 mL) was stirred at room temperature for 4 h. Subsequently, the reaction mixture was heated to 110 °C and refluxed for 4 h. Then, the resulting solution was poured into ice water (250 mL), and the pH value was adjusted to 9 by ammonia. The solid was filtrated and washed by water to afford intermediate **2** as pale yellow solid (13.22 g, yield 79.16%), which can be used directly in the next step without purification. ^1H NMR (DMSO, 500 MHz, ppm): δ 7.56 (m, 2H), 7.21 (m, 2H), 4.94 (s, 2H).

6.1.2. Chemical synthesis of *N*-((1H-benzimidazol-2-yl)methyl)hexan-1-amine (**3a**)

A solution of compound **2** (1.66 g, 0.01 mol) in MeOH (25 mL) was added dropwise to the suspension of hexan-1-amine (3.04 g, 0.03 mol) and anhydrous K_2CO_3 (2.76 g, 0.02 mol) in MeOH (10 mL). The mixture was stirred at room temperature for 0.5 h. The solvent was evaporated under reduced pressure. The residue was purified by column chromatography (CH_2Cl_2 : MeOH 100:2, v/v) to give **3a** as yellow oil (0.28 g, 12.1%). ^1H NMR (500 MHz, DMSO, TMS): δ 11.82 (w, 1H), 7.10–7.50 (m, 4H), 3.90 (s, 2H), 2.52 (m, 2H), 1.43 (m, 2H), 1.24 (m, 6H), 0.94 (t, 3H, $J = 7.0$ Hz). ^{13}C NMR (500 MHz, CDCl_3 , TMS): δ 147.32, 138.22, 122.96, 115.19, 47.97, 45.35, 31.17, 27.20, 26.37, 22.40, 13.83. MS (ESI) m/z : 232 ($M + 1$).

The synthetic procedure for the target compounds **3b–c**, **7a–c** and **10a–c** were similar to the synthesis of compound **3a**.

6.1.3. Chemical synthesis of ethyl 8-bromo-3,4-dihydro-1H-pyrido [4,3-b]indole -2(5H)-carboxylate (**17c**)

A solution of 4-bromophenylhydrazine hydrochloride (4.47 g, 0.02 mol) and 1-carbethoxy-4-piperidone (3.42 g, 0.02 mol) in EtOH (25 mL) was refluxed for 3 h. The reaction mixture was allowed to stand at room temperature overnight, and the solid product was collected by filtration, washed with 50% aqueous EtOH, and recrystallized from 95% EtOH to give **17c** as pale yellow solid (3.09 g, yield 47.5%). ¹H NMR (300 MHz, CDCl₃, TMS): δ7.27–7.88 (m, 3H), 4.66 (s, 2H), 4.21 (q, J = 7.2 Hz, 2H), 3.87 (br, 2H), 2.86 (br, 2H), 1.31 (t, J = 7.2 Hz, 3H). MS (ESI) m/z: 323 (M).

6.1.4. Chemical synthesis of ethyl 8-bromo-5-methyl-3,4-dihydro-1H-pyrido[4,3-b] indole-2(5H)-carboxylate (**18c**)

KOH (2.02 g, 0.036 mol) and CH₃I (7.10 g, 0.09 mol) was added to a solution of compound **11c** (2.96 g, 0.009 mol) in DMF (50 mL). The reaction mixture was stirred at room temperature for 12 h, then diluted with H₂O (100 mL) and extracted with ethyl acetate (50 mL × 3). The combined organic layers were washed with H₂O (100 mL × 3), dried over anhydrous Na₂SO₄, and filtrated, and the solvent was evaporated under reduced pressure. The residue was purified by silica gel column chromatography (hexane: EtOAc = 3:1, v/v) to give **18c** as pale yellow solid (0.41 g, yield 13.3%). ¹H NMR (300 MHz, DMSO, TMS): δ7.14–7.59 (m, 3H), 4.65 (s, 2H), 4.20 (dd, 2H, J₁ = 7.2 Hz, J₂ = 6.9 Hz), 3.89 (br, 2H), 3.63 (s, 3H), 2.83 (m, 2H), 1.31 (t, 3H, J = 7.0 Hz).

6.1.5. Chemical synthesis of 8-bromo-2-hexyl-5-methyl-2,3,4,5-tetrahydro-1H-pyrido[4,3-b]indole (**20g**)

A solution of compound **18c** (0.07 g, 0.26 mmol) in EtOH (10 mL) was added 1-bromohexane (0.17 g, 1.06 mmol) and anhydrous K₂CO₃ (0.15 g, 1.05 mmol). The reaction mixture was fluxed at 80 °C for 8 h. After filtration, the solvent was evaporated under reduced pressure. The residue was purified by column chromatography (CH₂Cl₂: MeOH 100:2, v/v) to give **20g** as brown oil (0.02 g, yield 22.2%). ¹H NMR (500 MHz, CDCl₃, TMS): δ7.09–7.52 (m, 3H), 3.64 (s, 2H), 3.58 (s, 3H), 2.87 (m, 2H), 2.83 (m, 2H), 2.59 (t, 2H, J = 7.7 Hz), 1.62 (m, 2H), 1.34 (m, 6H), 0.90 (t, 3H, J = 6.8 Hz). ¹³C NMR (500 MHz, CDCl₃, TMS): δ135.8, 135.4, 127.4, 123.2, 120.2, 112.1, 110.0, 107.6, 58.1, 50.6, 49.5, 31.8, 29.2, 27.6, 27.3, 22.9, 22.6, 14.0.

The synthetic methods for the target compounds **20a–o** were similar to the above procedure.

6.1.6. Chemical synthesis of 3-hexyl-6-methylquinazolin-4(3H)-one (**14a**)

NaH (60% oil, 0.8 g, 0.02 mol) was suspended to a solution of intermediate **13** (0.16 g, 0.01 mol) in DMF (10 mL), and the mixture was stirred at room temperature for 2 h. Then, 1-bromohexane (0.17 g, 0.01 mol) was added, the resulting mixture was heated to 80 °C and stirred for 9 h. After filtration, the solvent was evaporated under reduced pressure and the residue was purified by column chromatography (hexane: EtOAc = 4:1, v/v) to give **14a** as white solid (0.18 g, yield 75.0%). ¹H NMR (500 MHz, CDCl₃, TMS): δ8.11 (s, 1H), 7.56–8.02 (m, 3H), 4.00 (t, 2H, J = 7.4 Hz), 2.50 (s, 3H), 1.78 (m, 2H), 1.35 (m, 6H), 0.89 (t, 3H, J = 7.0 Hz). MS (ESI) m/z: 245 (M + 1).

The synthetic procedure for the target compounds **14b–c** was similar to the synthesis of compound **14a**.

6.1.7. N-((1H-benzimidazol-2-yl)methyl)heptan-1-amine (**3b**)

¹H NMR (500 MHz, DMSO, TMS): δ6.75–6.91 (m, 4H), 4.38 (s, 2H), 3.28 (m, 2H), 1.51 (m, 2H), 1.30 (m, 8H), 0.87 (t, 3H, J = 6.90 Hz). MS (ESI) m/z: 246 (M + 1).

6.1.8. N-((1H-benzimidazol-2-yl)methyl)octan-1-amine (**3c**)

¹H NMR (500 MHz, DMSO, TMS): δ12.22 (w, 1H), 7.10–7.48 (m, 4H), 3.88 (s, 2H), 2.50 (m, 2H), 1.43 (m, 2H), 1.26 (m, 10H), 0.85 (t, 3H, J = 6.9 Hz). MS (ESI) m/z: 260 (M + 1).

6.1.9. N-(benzoxazol-2-ylmethyl)hexan-1-amine (**7a**)

¹H NMR (500 MHz, DMSO, TMS): δ6.76–6.91 (m, 4H), 4.38 (s, 2H), 3.28 (m, 2H), 1.52 (m, 2H), 1.29 (m, 6H), 0.87 (t, 3H, J = 6.9 Hz).

6.1.10. N-(benzoxazol-2-ylmethyl)heptan-1-amine (**7b**)

¹H NMR (500 MHz, DMSO, TMS): δ6.76–6.91 (m, 4H), 4.38 (s, 2H), 3.28 (m, 2H), 1.52 (m, 2H), 1.29 (m, 8H), 0.87 (t, 3H, J = 6.9 Hz). MS (ESI) m/z: 247 (M + 1).

6.1.11. N-(benzoxazol-2-ylmethyl)octan-1-amine (**7c**)

¹H NMR (500 MHz, DMSO, TMS): δ6.76–6.91 (m, 4H), 4.38 (s, 2H), 3.28 (m, 2H), 1.52 (m, 2H), 1.29 (m, 10H), 0.86 (t, 3H, J = 6.9 Hz). ¹³C NMR (500 MHz, CDCl₃, TMS): δ154.06, 145.45, 135.43, 124.17, 123.20, 122.65, 115.19, 67.33, 63.06, 40.82, 31.77, 29.78, 29.25, 26.97, 22.61, 14.05. MS (ESI) m/z: 261 (M + 1).

6.1.12. N-(benzothiazol-2-ylmethyl)hexan-1-amine (**10a**)

¹H NMR (500 MHz, DMSO, TMS): δ7.36–8.05 (m, 4H), 4.08 (s, 2H), 2.88 (s, 1H), 2.59 (t, 2H), 1.45 (m, 2H), 1.29 (m, 6H), 0.86 (t, 2H, J = 7.0 Hz). MS (ESI) m/z: 249 (M + 1).

6.1.13. N-(benzothiazol-2-ylmethyl)heptan-1-amine (**10b**)

¹H NMR (500 MHz, DMSO, TMS): δ7.37–8.05 (m, 4H), 4.08 (s, 2H), 2.76 (s, 1H), 2.59 (t, 2H, J = 7.0 Hz), 1.46 (m, 2H), 1.29 (m, 8H), 0.85 (t, 3H, J = 6.8 Hz). MS (ESI) m/z: 263 (M + 1).

6.1.14. N-(benzothiazol-2-ylmethyl)octan-1-amine (**10c**)

¹H NMR (500 MHz, DMSO, TMS): δ7.37–8.05 (m, 4H), 4.08 (s, 2H), 2.59 (t, 2H, J = 7.0 Hz), 1.44 (m, 2H), 1.29 (m, 10H), 0.85 (t, 3H, J = 6.9 Hz). MS (ESI) m/z: 277 (M + 1).

6.1.15. 3-Heptyl-6-methylquinazolin-4(3H)-one (**14b**)

¹H NMR (500 MHz, CDCl₃, TMS): δ8.11 (s, 1H), 7.56–7.98 (m, 3H), 3.99 (t, 2H, J = 7.4 Hz), 2.50 (s, 3H), 1.78 (m, 2H), 1.35 (m, 8H), 0.89 (t, 3H, J = 7.0 Hz). MS (ESI) m/z: 259 (M + 1).

6.1.16. 3-Octyl-6-methylquinazolin-4(3H)-one (**14c**)

¹H NMR (500 MHz, CDCl₃, TMS): δ8.10 (s, 1H), 7.56–7.98 (m, 3H), 3.99 (t, 2H, J = 7.4 Hz), 2.50 (s, 3H), 1.78 (m, 2H), 1.34 (m, 10H), 0.89 (t, 3H, J = 7.0 Hz). ¹³C NMR (500 MHz, CDCl₃, TMS): δ161.03, 146.13, 145.79, 137.39, 135.50, 127.18, 126.08, 121.91, 46.99, 31.69, 29.38, 29.09, 26.64, 22.56, 21.08, 14.00. MS (ESI) m/z: 273 (M+1).

6.1.17. 8-Fluoro-2-hexyl-5-methyl-2,3,4,5-tetrahydro-1H-pyrido [4,3-b]indole (**20a**)

¹H NMR (500 MHz, CDCl₃, TMS): δ6.86–7.25 (m, 3H), 3.74 (s, 2H), 3.60 (s, 3H), 2.95 (m, 2H), 2.87 (m, 2H), 2.65 (t, 2H, J = 7.6 Hz), 1.66 (m, 2H), 1.34 (m, 6H), 0.89 (t, 3H, J = 7.0 Hz). MS (ESI) m/z: 290 (M).

6.1.18. 8-Fluoro-2-heptyl-5-methyl-2,3,4,5-tetrahydro-1H-pyrido [4,3-b]indole (**20b**)

¹H NMR (500 MHz, CDCl₃, TMS): δ6.87–7.15 (m, 3H), 3.64 (s, 2H), 3.60 (s, 3H), 2.88 (m, 2H), 2.85 (m, 2H), 2.60 (t, 2H, J = 7.7 Hz), 1.63 (m, 2H), 1.29–1.35 (m, 8H), 0.89 (t, 3H, J = 7.0 Hz). MS (ESI) m/z: 303 (M + 1).

6.1.19. 8-Fluoro-5-methyl-2-octyl-2,3,4,5-tetrahydro-1H-pyrido [4,3-b]indole (**20c**)

¹H NMR (500 MHz, CDCl₃, TMS): δ6.86–7.14 (m, 3H), 3.64 (s, 2H), 3.59 (s, 3H), 2.92 (m, 2H), 2.83 (m, 2H), 2.59 (t, 2H, J = 7.7 Hz), 1.62 (m, 2H), 1.27–1.34 (m, 10H), 0.89 (t, 3H, J = 7.0 Hz). MS (ESI) m/z: 319 (M + 1).

6.1.20. 8-Chloro-2-hexyl-5-methyl-2,3,4,5-tetrahydro-1H-pyrido[4,3-b]indole (**20d**)

¹H NMR (500 MHz, CDCl₃, TMS): δ7.07–7.36 (m, 3H), 3.65 (s, 2H), 3.59 (s, 3H), 2.89 (m, 2H), 2.84 (m, 2H), 2.60 (t, 2H, *J* = 7.7 Hz), 1.63 (m, 2H), 1.35 (m, 6H), 0.90 (t, 3H, *J* = 6.7 Hz).

6.1.21. 8-Chloro-2-heptyl-5-methyl-2,3,4,5-tetrahydro-1H-pyrido[4,3-b]indole (**20e**)

¹H NMR (500 MHz, CDCl₃, TMS): δ7.06–7.36 (m, 3H), 3.65 (s, 2H), 3.58 (s, 3H), 2.88 (m, 2H), 2.83 (m, 2H), 2.60 (t, 2H, *J* = 7.7 Hz), 1.62 (m, 2H), 1.30–1.35 (m, 8H), 0.89 (t, 3H, *J* = 6.8 Hz).

6.1.22. 8-Chloro-5-methyl-2-octyl-2,3,4,5-tetrahydro-1H-pyrido[4,3-b]indole (**20f**)

¹H NMR (500 MHz, CDCl₃, TMS): δ7.07–7.36 (m, 3H), 3.65 (s, 2H), 3.59 (s, 3H), 2.88 (m, 2H), 2.83 (m, 2H), 2.60 (t, 2H, *J* = 7.7 Hz), 1.62 (m, 2H), 1.29–1.34 (m, 10H), 0.89 (t, 3H, *J* = 6.9 Hz).

6.1.23. 8-Bromo-2-heptyl-5-methyl-2,3,4,5-tetrahydro-1H-pyrido[4,3-b]indole (**20h**)

¹H NMR (500 MHz, CDCl₃, TMS): δ7.09–7.52 (m, 3H), 3.64 (s, 2H), 3.58 (s, 3H), 2.83 (m, 2H), 2.88 (m, 2H), 2.59 (t, 2H, *J* = 7.8 Hz), 1.63 (m, 2H), 1.26–1.35 (m, 8H), 0.89 (t, 3H, *J* = 6.9 Hz).

6.1.24. 8-Bromo-5-methyl-2-octyl-2,3,4,5-tetrahydro-1H-pyrido[4,3-b]indole (**20i**)

¹H NMR (500 MHz, CDCl₃, TMS): δ7.09–7.52 (m, 3H), 3.64 (s, 2H), 3.58 (s, 3H), 2.88 (m, 2H), 2.83 (m, 2H), 2.59 (t, 2H, *J* = 7.7 Hz), 1.62 (m, 2H), 1.29–1.34 (m, 10H), 0.89 (t, 3H, *J* = 6.8 Hz).

6.1.25. 8-Iodo-2-hexyl-5-methyl-2,3,4,5-tetrahydro-1H-pyrido[4,3-b]indole (**20j**)

¹H NMR (500 MHz, CDCl₃, TMS): δ7.01–7.73 (m, 3H), 3.64 (s, 2H), 3.58 (s, 3H), 2.88 (m, 2H), 2.83 (m, 2H), 2.59 (t, 2H, *J* = 7.7 Hz), 1.62 (m, 2H), 1.34 (m, 6H), 0.90 (t, 3H, *J* = 6.8 Hz).

6.1.26. 8-Iodo-2-heptyl-5-methyl-2,3,4,5-tetrahydro-1H-pyrido[4,3-b]indole (**20k**)

¹H NMR (500 MHz, CDCl₃, TMS): δ7.01–7.72 (m, 3H), 3.65 (s, 2H), 3.58 (s, 3H), 2.89 (m, 2H), 2.84 (m, 2H), 2.60 (t, 2H, *J* = 7.7 Hz), 1.63 (m, 2H), 1.29–1.35 (m, 8H), 0.89 (t, 3H, *J* = 6.9 Hz).

6.1.27. 8-Iodo-5-methyl-2-octyl-2,3,4,5-tetrahydro-1H-pyrido[4,3-b]indole (**20l**)

¹H NMR (500 MHz, CDCl₃, TMS): δ7.00–7.72 (m, 3H), 3.63 (s, 2H), 3.57 (s, 3H), 2.87 (m, 2H), 2.82 (m, 2H), 2.58 (t, 2H, *J* = 7.7 Hz), 1.62 (m, 2H), 1.28–1.33 (m, 10H), 0.89 (t, 3H, *J* = 7.0 Hz). ¹³C NMR (500 MHz, CDCl₃, TMS): δ136.2, 135.0, 128.7, 128.2, 126.4, 110.6, 107.4, 82.1, 58.1, 50.7, 49.4, 31.8, 29.6, 29.2, 27.6, 22.8, 22.6, 14.1.

6.1.28. 2-Hexyl-5,8-dimethyl-2,3,4,5-tetrahydro-1H-pyrido[4,3-b]indole (**20m**)

¹H NMR (500 MHz, CDCl₃, TMS): δ6.96–7.19 (m, 3H), 3.95 (s, 2H), 3.58 (s, 3H), 2.88 (m, 2H), 2.83 (m, 2H), 2.60 (t, 2H, *J* = 7.8 Hz), 2.43 (s, 3H), 1.63 (m, 2H), 1.32 (m, 6H), 0.90 (t, 3H, *J* = 6.9 Hz).

6.1.29. 2-Heptyl-5,8-dimethyl-2,3,4,5-tetrahydro-1H-pyrido[4,3-b]indole (**20n**)

¹H NMR (500 MHz, CDCl₃, TMS): δ6.96–7.19 (m, 3H), 3.66 (s, 2H), 3.58 (s, 3H), 2.90 (m, 2H), 2.83 (m, 2H), 2.61 (t, 2H, *J* = 7.8 Hz), 2.43 (s, 3H), 1.63 (m, 2H), 1.29–1.35 (m, 8H), 0.89 (t, 3H, *J* = 7.0 Hz).

6.1.30. 2-Octyl-5,8-dimethyl-2,3,4,5-tetrahydro-1H-pyrido[4,3-b]indole (**20o**)

¹H NMR (500 MHz, CDCl₃, TMS): δ6.95–7.19 (m, 3H), 3.68 (s, 2H), 3.57 (s, 3H), 2.88 (m, 2H), 2.82 (m, 2H), 2.60 (t, 2H, *J* = 7.7 Hz), 2.43 (s, 3H, CH₃), 1.63 (m, 2H), 1.28–1.34 (m, 10H), 0.89 (t, 3H, *J* = 6.9 Hz). ¹³C NMR (500 MHz, CDCl₃, TMS): δ135.5, 133.9, 127.8, 125.9, 122.0, 117.3, 108.3, 107.2, 58.1, 50.9, 49.7, 31.8, 29.6, 29.3, 29.0, 27.7, 22.8, 22.6, 14.1.

6.2. Flexible molecular docking

The 3D structure of CACYP51 was obtained by homology modeling [9]. Flexible ligand docking procedure in the Affinity module within InsightII was used to define the lowest energy position for the substrate using a Monte Carlo docking protocol. The detailed docking parameters were from our previous studies [17].

Acknowledgment

This work was supported by the National Natural Science Foundation of China (Grant Nos. 30930107, 30973640), Shanghai Rising-Star Program (Grant Nos. 09QA1407000) and Shanghai Leading Academic Discipline Project (Project Nos. B906).

References

- [1] J.J. Caston-Osorio, A. Rivero, J. Torre-Cisneros, *Int. J. Antimicrob. Agents* 32 (Suppl. 2) (2008) S103–109.
- [2] M. Cuenca-Estrella, L. Bernal-Martinez, M.J. Buitrago, M.V. Castelli, A. Gomez-Lopez, O. Zaragoza, J.L. Rodriguez-Tudela, *Int. J. Antimicrob. Agents* 32 (Suppl. 2) (2008) S143–147.
- [3] Y. Aoyama, Y. Yoshida, R. Sato, *J. Biol. Chem.* 259 (1984) 1661–1666.
- [4] R.A. Fromtling, *Clin. Microbiol. Rev.* 1 (1988) 187–217.
- [5] J.T. Slama, J.L. Hancock, T. Rho, L. Sambucetti, K.A. Bachmann, *Biochem. Pharmacol.* 55 (1998) 1881–1892.
- [6] J. Peman, E. Canton, A. Espinel-Ingroff, *Expert Rev. Anti. Infect. Ther.* 7 (2009) 453–460.
- [7] H. Ji, W. Zhang, Y. Zhou, M. Zhang, J. Zhu, Y. Song, J. Lu, *J. Med. Chem.* 43 (2000) 2493–2505.
- [8] C. Sheng, Z. Miao, H. Ji, J. Yao, W. Wang, X. Che, G. Dong, J. Lu, W. Guo, W. Zhang, *Antimicrob. Agents Chemother.* 53 (2009) 3487–3495.
- [9] C. Sheng, W. Wang, X. Che, G. Dong, S. Wang, H. Ji, Z. Miao, J. Yao, W. Zhang, *Chem. Med. Chem.* 5 (2010) 390–397.
- [10] C. Sheng, W. Zhang, M. Zhang, Y. Song, H. Ji, J. Zhu, J. Yao, J. Yu, S. Yang, Y. Zhou, J. Lu, *J. Biomol. Struct. Dyn.* 22 (2004) 91–99.
- [11] H. Ji, W. Zhang, M. Zhang, M. Kudo, Y. Aoyama, Y. Yoshida, C. Sheng, Y. Song, S. Yang, Y. Zhou, J. Lu, J. Zhu, *J. Med. Chem.* 46 (2003) 474–485.
- [12] C.A. Harbert, J.J. Plattner, W.M. Welch, A. Weissman, B.K. Koe, *J. Med. Chem.* 23 (1980) 635–643.
- [13] N. Khorana, A. Purohit, K. Herrick-Davis, M. Teitler, R.A. Glennon, *Bioorg. Med. Chem.* 11 (2003) 717–722.
- [14] B. Yao, H. Ji, Y. Cao, Y. Zhou, J. Zhu, J. Lu, Y. Li, J. Chen, C. Zheng, Y. Jiang, R. Liang, H. Tang, *J. Med. Chem.* 50 (2007) 5293–5300.
- [15] H. Zhao, *Drug Discov. Today* 12 (2007) 149–155.
- [16] S.D. InsightII 2000. Molecular Simulation Inc, 9685 Scranton Road, CA 92121-3752, 1999.
- [17] C. Sheng, W. Zhang, H. Ji, M. Zhang, Y. Song, H. Xu, J. Zhu, Z. Miao, Q. Jiang, J. Yao, Y. Zhou, J. Lu, *J. Med. Chem.* 49 (2006) 2512–2525.